MIMOSA Research Note No.

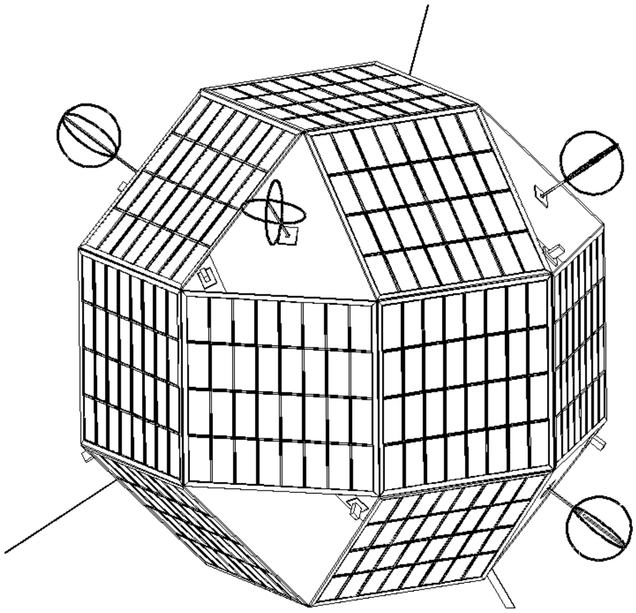

Attitude determination and the satellite's cross-section

Prepared by: Doc. RNDr. David Vokrouhlický, DrSc.

Prague, Dec 2000

Contents

1 Introduction

The purpose of this research note is twofold:

- based on a macroscopic model of the MIMOSA shape, to compute the interval of possible values of its effective cross-section and to derive a distribution of probability for this quantity under different situations, and
- to discuss a method, and to test a software, that should allow attitude determination of the satellite from measurements performed by the optical sensors and the magnetometer.

Both items represent necessary information for a precise evaluation of the atmospheric density from the measurements of the accelerometer MACEK (on board of MIMOSA).

Assuming a hyperthermal flow of the atmospheric particles (i.e. the mean thermal velocity of the atmospheric components much smaller that the satellite orbital velocity), one may approximate acceleration $d\mathbf{f}$ exerted on a surface element $d\mathbf{S} = \mathbf{n}\, dS$ of the satellite by (e.g. King-Hele 1964, Beletskii and Yanshin 1984)

$$d\mathbf{f} = (\mathbf{e}_V \cdot d\mathbf{S})\, \frac{\rho V^2}{m} \left\{ (1-\epsilon)\, \mathbf{e}_V + 2\epsilon\, (\mathbf{e}_V \cdot \mathbf{n})\, \mathbf{n} + (1-\epsilon)\, \frac{v_t}{V} \mathbf{n} \right\} \; . \tag{1}$$

Here, $V = V\, \mathbf{e}_V$ is the mean velocity of the atmospheric flow in the body-fixed frame of the satellite (composed from the translational motion of the satellite around the Earth and the rotation of the atmosphere; rotation of the satellite may be neglected), ρ is the mean density of the atmosphere and m is the mass of the satellite. The complicated microphysics of the interaction of the satellite surface with the atmospheric components is enclosed, at this level of approximation, in two parameters: (i) ϵ is a fraction of molecules that are reflected specularly from the surface, and (ii) v_t is the effective, mean thermal velocity of the diffusely reflected molecules (in the body-fixed frame of the spacecraft). Hereafter, we shall not discuss the complex issue of possible dependence of both ϵ and v_t on the incidence angle of the flow on the surface element and the relative velocity V (and we relegate it to a subsequent text; see also Sehnal 1982, Harrison and Swinerd 1995). Similarly, at a high level of precision one should also account for the effects of the “finite” (and nonzero) thermal velocity of the atmospheric components. At the altitude of about 500 km the mean atmospheric temperature may be ≈ 1000 K and which implies, assuming the mean molecular weight of about 18 at that altitude, the mean thermal velocity ≈ 1 km/s. The spacecraft orbital velocity is thus larger only by a factor of ≈ 5. The finite thermal velocity corrections to the expression of $d\mathbf{f}$ are rather algebraically complicated (e.g. Beletskii and Yanshin 1984, Klinkrad et al. 1999), and their detailed discussion is relegated to the forthcoming note.

Here, we assume for illustration ϵ and v_t constant, or at least given function of V only, and the total acceleration then reads

$$\mathbf{f} = \int_{S_+} d\mathbf{f} \; . \tag{2}$$

The integral in (2) is performed over surface elements with $\mathbf{e}_V \cdot \mathbf{n} \leq 0$. Conventionally, one introduces a drag coefficient C_D so that the along-velocity component of the acceleration (2) is given by the following formula

$$\mathbf{f}_D = \frac{C_D}{2} \, \rho V^2 \, \frac{S}{m} \, \mathbf{e}_V \; , \tag{3}$$

and S is the cross-section of the satellite. For a spherical satellite this is the only component of the acceleration and

$$C_D \simeq 2 \left[1 + \frac{2}{3} \frac{v_t}{V} \, (1 - \epsilon) \right] \tag{4}$$

might be a weakly dependent function of the velocity V (through dependence of ϵ and v_t on V). For a highly symmetric satellite like MIMOSA, we may still assume (4) to be correct at a first approximation. To relate the measured accelerations $\approx \mathbf{f}_D$ to the information about density ρ, one must know the cross-section S of the satellite and one must assume some value of the C_D coefficient. Uncertainty in C_D is obviously a delicate task of any determination procedure. As a first approximation one may assume the C_D coefficient to be constant and solved-for parameter, if a large number observations at approximately same altitude are considered (i.e. they would have thus similar relative velocity of the satellite with respect to the atmosphere). In addition, a long-term time-dependence of C_D may be considered due to space weathering effects (e.g. Sehnal 1982).

Similarly, determination of the radiation pressure on the spacecraft due to the direct sunlight or sunlight reflected on the Earth (the albedo effect), requires knowledge of the cross-section of the spacecraft in the corresponding direction. The radiation pressure on a surface element $d\mathbf{S}$ of the satellite can be expressed as in (1) with changing $\rho V^2 \to \Phi/c$ (Φ is the radiation flux and c the light velocity) and $v_t/V \approx 1$. With similar changes done, the formula (3) thus approximates the total radiation pressure exerted on a highly symmetric satellite (here $\mathbf{e}_V$ is opposite to the direction to the Sun).

Theoretical determination of the satellite acceleration due to both the atmospheric and radiation effects thus involve at some stage knowledge of its cross-section along a given direction. Though of rather regular shape, MIMOSA's cross-section is not exactly constant along all possible directions. This yields motivation to determine attitude of the satellite and thus be able to compute its cross-section.

2 Cross-section of MIMOSA - a first estimate

Hereafter, we shall estimate the most likely value of the MIMOSA cross-section (which may be then used as a zero-level approximation in (3)). For this purpose, we use the macroscopic shape model by Bourek (2000), where MIMOSA is approximated by 26 surface planar elements.

As a first glimpse of the problem, we compute cross-section of MIMOSA as a function of the tilt θ from the symmetry axis ($\mathbf{e}_z$) of the satellite – Figure 1. We have chosen $S_1 = 0.22^2 = 0.0484$ m^2 as unit of the area (this is the area of the rectangular surface elements). The crucial information to be learnt from this figure is an estimation of the difference between the minimum and maximum values of the computed cross-section: taking 4.83 and 5.4 for the lower and upper values we have at maximum 11.8 % variation of the satellite cross-section.

Next, we have to substantiate the previous result by understanding whether all values between the estimated minimum and maximum values of the cross-section are equally likely to occur. This task involves an assumption about the distribution of the unit vectors $\mathbf{e}_V$ along which the atmospheric molecules inflow on the satellite. This information may, in principle, be a complicated function of the rotation state of the satellite (and its relation to the spacecraft revolution around the Earth). The work of Bourek (2000) indicated that MIMOSA (similarly to CASTOR/CACTUS) will likely be captured in a higher order spin-orbit resonance state, showing probably a chaotic rotation. In this situation, we may consider an isotropic distribution of the $\mathbf{e}_V$ vectors as a good approximation and we determine numerically the (normalized) distribution function $f(S)$ that gives probability $dp = f(S)\,dS$ of states with the cross-section between S and $S + dS$.

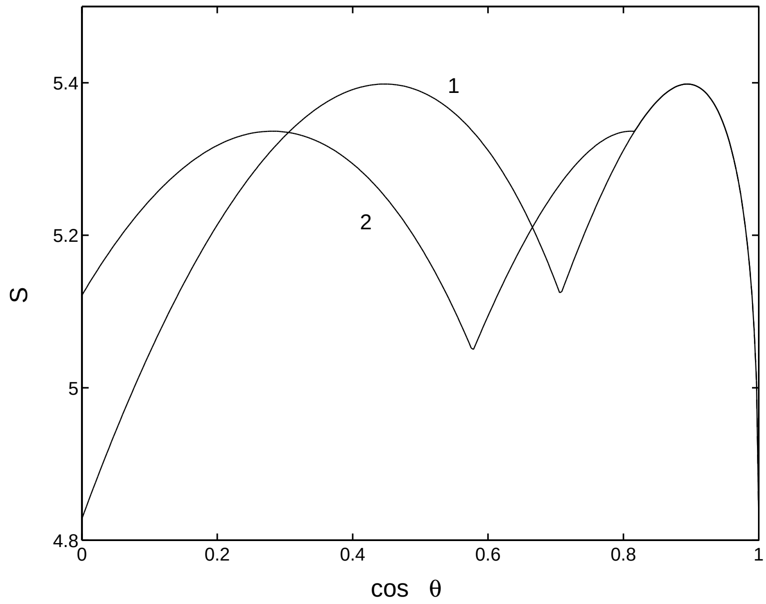

Figure 1: Cross-section of MIMOSA (S given in units of $S_1 = 0.0484$ m^2) as a function of the tilt angle θ from the satellite symmetry axis $\mathbf{e}_z$; 26-element macro-model of Bourek (2000) used. Curve 1 gives the cross-section for seeing vectors in the $\mathbf{e}_x - \mathbf{e}_z$ plane, curve 2 for seeing vectors in the plane rotated by 45 degrees.

Figure 2 shows $f(S)$ computed from a random shooting a million values of $\mathbf{e}_V$ (here f has been normalized to its maximum value). We may notice a sharp maximum at $S \approx 5.42$ and a high deficiency of cross-sections smaller than ≈ 5.2; the distribution is non-uniform. The shaded area indicates an interval of the cross-sections around the maximum of $f(S)$ that has 50 % likelihood.

We may thus conclude that, choosing a random direction in space, the satellite's cross-section will span with high probability much smaller interval than that delimited by the extreme values 4.8 – 5.5. If nothing is known about the satellite orientation, we may thus adopt a nominal cross-section value of $5.42\, S_1 \simeq 0.2623$ m^2 ($S_1 = 0.22^2 = 0.0484$ m^2). Assuming $C_D \approx 2$ we then obtain an estimate of the typical atmospheric drag $f_D \approx 2.4 \times 10^{-5}\, \rho_{10}$ m/s^2, where ρ_{10} is the atmospheric density in 10^{-10} kg/m^3 (this is

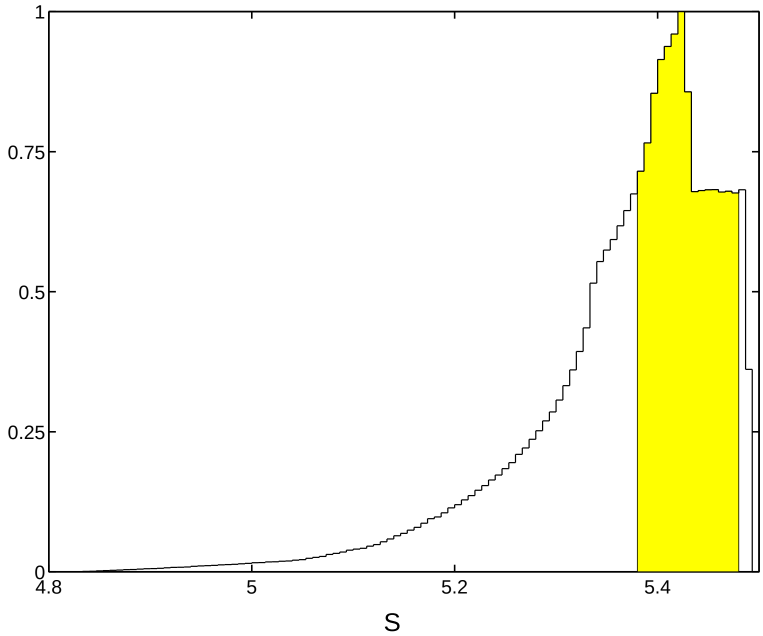

Figure 2: Distribution function $f(S)$ of MIMOSA cross-section S (S given in units of $S_1 = 0.0484$ m^2). Random distribution of the incident directions along which the atmospheric molecules impact the satellite assumed. The shaded area shows a 50 % likelihood interval of cross-sections near the maximum at ≈ 5.42.

about a maximum density for altitudes higher than 300 km).

As it will be mentioned in Section 3, MIMOSA will dispose of an on-board attitude-monitoring system. Its part consist in several optical sensors on the satellite surface, that should be able to determine rather precisely direction toward the Sun. This information is relevant for computation of the spacecraft cross-section with respect to the solar radiation, and thus for determination of the corresponding radiation pressure. Obviously, this information is not enough to know the satellite cross-section along its velocity and position vector directions, that are relevant for computation of the atmospheric and albedo accelerations. We devote Section 3 for a discussion of these, more complicated, issues. In what follows, we shall estimate how the uncertainties in the measurements of the direction toward the Sun

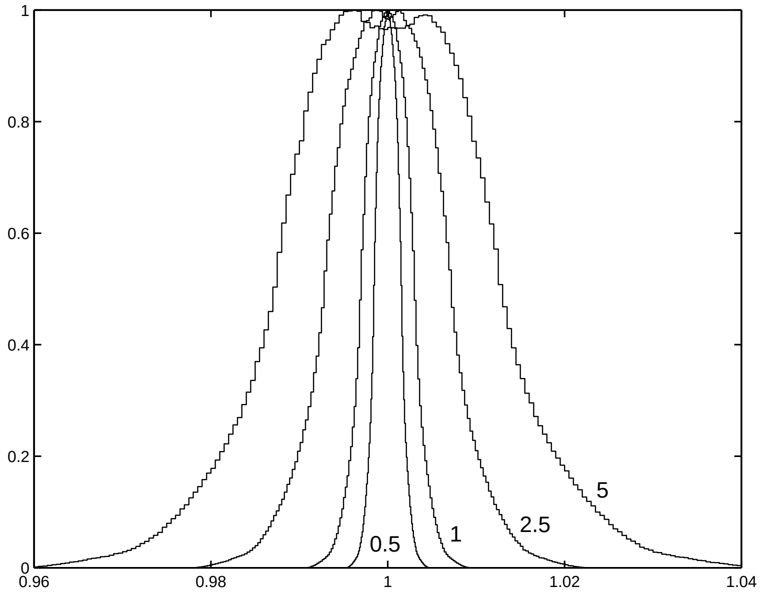

Figure 3: Ratio of the biased and the "true" cross-section of MIMOSA as referred to the direction toward the Sun (and thus relevant for the determination of the radiation acceleration due to sunlight). The biased cross-section results from uncertainty in the on-board measurement of the direction toward the Sun (by the system of the optical sensors). We assume that the measured directions are systematically wrong by some tilt-angle from the true direction. Four values of the tilt-angle considered (labels along the curves): 0.5, 1, 2.5 and 5 degrees.

(by the surface optical sensors) affect the corresponding determination of the satellite's cross-section along this (measured) direction. According to the technical documentation in the *Report for the Grant Agency (1998)* the expected uncertainty of the optical system in the body-fixed frame should be about 0.5 degree. As a pessimistic assumption, we shall also test results with errors up to 5 degrees in the solar direction determination. To be really conservative, we performed the following test. First, we selected randomly a "true" orientation toward the Sun and we computed the "true" cross-section of the satellite with respect to this direction. Next, we assumed that the on-board attitude-determination system fails to determine the true direction toward the Sun by a certain (constant) angle – 0.5, 1, 2.5 and 5 degrees. We randomly selected a direction tilt from the true direction toward the Sun by this angle and determined the spacecraft cross-section with respect to the measured (but biased) direction toward the Sun. Then we compute ratio R of the biased and true cross-sections. Obviously, we repeated this procedure large number of times choosing random orientation of the true direction toward the Sun. Distribution of r for a five million of trials is shown in Figure 3. We may notice, that even in the worst case – a systematic 5 degree bias between the true and measured directions toward the Sun, the spacecraft cross-section is still determined with about 2 % half-width error. If we assume better performance of the optical-sensor system, the relative error in determination of the satellite cross-section drops below 1 %. This is fairly satisfactory for determination of the direct solar radiation pressure, since the error in the cross-section will be probably less that the uncertainty in our knowledge of the reflectivity properties of the satellite surface.

3 Attitude determination

The previous exercise represented a global information about the possible values of the satellite cross-section and their likelihood analysis. However, at a higher level of understanding we should ideally know at any instant the orientation of the satellite in space and compute the cross-section along an arbitrary direction. For that purpose the MIMOSA project disposes of the attitude control system, consisting of (i) the optical sensors at the surface (mentioned above), and (ii) the magnetometer. Both of these two segments serve to determine a body-fixed orientation of one of the two unit vectors: direction toward the Sun and direction of the geomagnetic field. At a given epoch (i.e. position and velocity of the satellite) we obviously know also directions of these two vectors in the inertial frame. As a result, the attitude determination reduces to solving for the rotation parameters of the body-fixed frame (with respect to the inertial frame) from knowing coordinates of two vectors in both frames. Note that if only direction of one vector is known in the two frames, the spacecraft orientation cannot be solved since rotation about this vector is not constrained. This situation happens when the satellite gets in the Earth shadow and the solar direction cannot be resolved from the optical-monitoring system. For that purpose Bourek (2000) attempted to construct a numerical model of evolution of the MIMOSA rotation state.

Motivated by the practical problem mentioned above, we shall hereafter describe a possible method for solving the spacecraft orientation from two vectors known in both the inertial and body-fixed frames (and thus not referring at any instant to theoretical model of satellite's rotation). Obviously, since the measurements are subjected to uncertainties we have to analyse how they will affect the attitude determination procedure. This is actually the primary goal of the following text. As it has been mentioned above, according to the technical documentation in the *Report for the Grant Agency (1998)* the expected uncertainty of the optical and magnetometer system in the body-fixed frame should be about half-degree. The inertial frame directions of the same vectors should be known with a much better precision (and here we shall thus neglect the inertial frame uncertainties).

In principle, the necessary mathematical background is enclosed in a simple equation

$$\mathbf{V}' = \mathcal{A} \cdot \mathbf{V} \ , \tag{5}$$

where $\mathbf{V}'$ and $\mathbf{V}$ is a vector given in the body-fixed and inertial frames (the body-fixed variables will be primed); $\mathcal{A}$ is the orthonormal matrix of the coordinate transformation. Nine components of the matrix $\mathcal{A}$ are constrained by six equations $\mathcal{A}_{ik}\mathcal{A}_{jk} = \delta_{ij}$. Though we may work directly with the matrix $\mathcal{A}$, and thus fully characterize at every instant rotation between the inertial and the body-fixed frames, the over-parameterization (due to large number of constraints on the solved-for parameters) is sometimes not suitable. Moreover, since our ambition is to develop also a numerical model for description of the satellite rotation (motivated mainly by a failure of the measuring system in the Earth shadow; see above and for the theoretical model of the satellite rotation Bourek 2000), we need to observationally determine the same set of parameters that we use in the dynamical theory of the satellite rotation.

The whole problem then consists in choosing a suitable parameterization of the rotation between the two frames (i.e. technically the elements of the matrix $\mathcal{A}$). This classical task has been considered many times in the past (see, e.g., Mignard 1990, Koshlyakov 1985). Bourek (2000) used the set of Euler angles (ψ, θ, ϕ) to characterize the rotation between the inertial and body-fixed frames. This is the choice where minimum number of parameters appears (3 with no constrains), but it is also well known that it suffers some "coordinate" inconveniences when the nutation angle θ becomes small. We shall illustrate this property in Section 3.1, where we discuss a possibility to parametrize the rotation matrix $\mathcal{A}$ by the set of Euler angles. Rotation between two coordinate frames may be sometimes more conveniently parametrized by other sets of quantities (e.g. the Cayley-Klein parameters, see Mignard 1990). However, we relegate these more complex possibilities to further development of our approach.

3.1 Euler representation and its determination

The classical Euler angle parameterization of $\mathcal{A}$ reads

$$\mathcal{A} = \begin{pmatrix} \cos\psi\cos\phi - \sin\psi\sin\phi\cos\theta & \cos\phi\sin\psi + \sin\phi\cos\psi\cos\theta & \sin\phi\sin\theta \\ -\sin\phi\cos\psi - \cos\phi\sin\psi\cos\theta & -\sin\phi\sin\psi + \cos\phi\cos\psi\cos\theta & \cos\phi\sin\theta \\ \sin\psi\sin\theta & -\cos\psi\sin\theta & \cos\theta \end{pmatrix} . \quad (6)$$

Note that we use the "3-1-3" sequence of rotations, corresponding to the definition of the precession, nutation and proper rotation (see Mignard 1990). Inversely, had we determined components of the matrix $\mathcal{A}$ we have

$$\theta = \mathrm{acos}\ (\mathcal{A}_{33}) , \quad (7)$$
$$\phi = \mathrm{atan2}\,(\mathcal{A}_{13}, \mathcal{A}_{23}) , \quad (8)$$
$$\psi = \mathrm{atan2}\,(\mathcal{A}_{31}, -\mathcal{A}_{32}) \quad (9)$$

for the Euler angles ("Fortran-command notation used here").

As a first test, we have fixed the satellite frame to be characterized by the following set of Euler angles (as referred to the inertial space): $\psi = 73$ degrees, $\theta = 23$ degrees, and $\phi = 235$ degrees (these values were obviously chosen randomly; similar results would be obtained if another set of parameters is considered). Then, we randomly chose position vector of the Sun and direction of the geomagnetic field in the inertial system and transformed them into the body-fixed frame. These transformed vectors were then biased in order to simulate uncertainty in the optical-sensors and the magnetometer

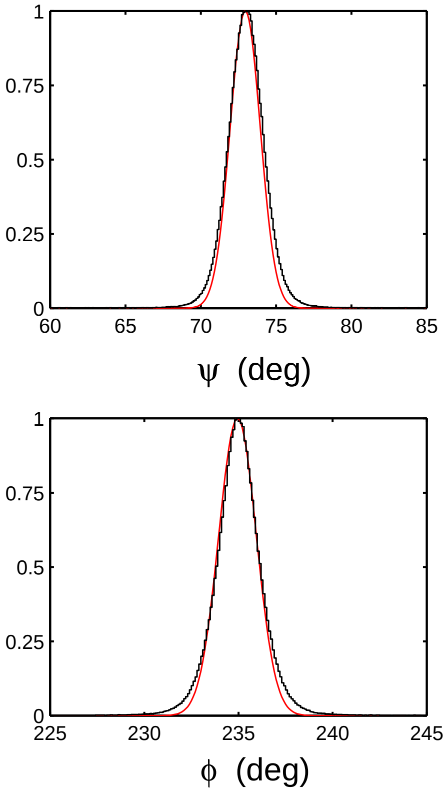

Figure 4: Statistical properties of the spacecraft attitude solution from the on-board monitoring of two vectors known in the inertial frame (e.g. direction to the Sun and direction of the geomagnetic field). Euler-angle parameterization of the rotation between the inertial and body-fixed frames assumed. The uncertainty of the on-board measurements is modelled as gaussian with 0.5 degrees standard deviation and the admittance level $\epsilon = 0.01$ (see the text). When the nutation angle is not small (here $\theta = 23$ degrees is the correct value) the solution is good, with only slightly worse statistics of the solution in the precession angle ψ and the angle of proper rotation ϕ (they can be approximated by gaussian with ≈ 1.5 degree standard deviations; light curves).

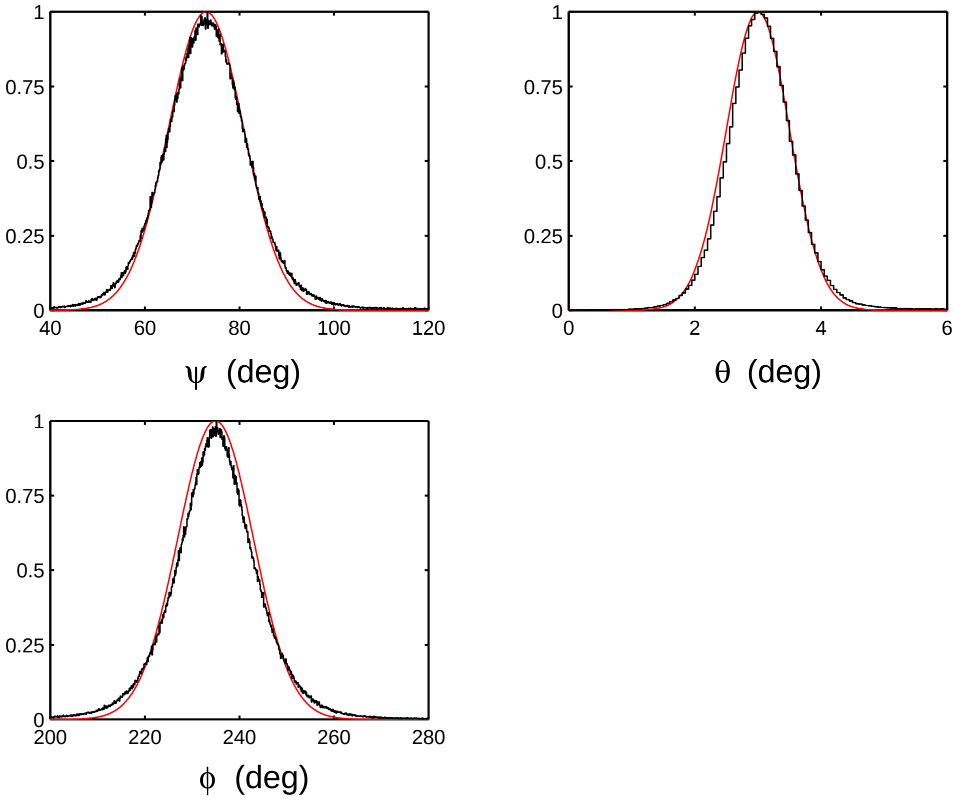

Figure 5: The same as in the Figure 4 but here the correct value of the nutation angle θ has been decreased to 3 degrees. Resolution in θ is still good (0.5 degrees standard deviation approximately), but solution for the precession angle ψ and the angle of proper rotation ϕ are much degraded (up to ≈ 8 degrees standard deviation distribution).

measurements. We considered gaussian noise with the standard deviation of 0.5 degree. Now, having the precise knowledge of the solar direction and direction of the magnetic field in the inertial frame *and* knowledge of the corresponding, but biased, vectors in the body-fixed frame of the spacecraft we tried to reconstruct the (a priori known) rotation parameters (ψ, θ, ϕ). We then repeated this procedure for a large number of randomly chosen position vectors of the Sun and the geomagnetic field. Since the body-fixed direction vectors are biased, the attitude-determination procedure may not necessarily converge with a specified precision of the process. To quantify this effect we have to explain in some detail the algorithm we use for determination of the Euler angles. First, we do not solve-for the Euler angles directly but we determine elements of the rotation matrix $\mathcal{A}$ by involving the definition (5) for the two measured/known vectors. Since (5) yields 6 algebraic equations for 9 unknown elements of $\mathcal{A}$ we must involve 3 of the 6 constraints. Notably we employ unitary properties of the rows: $\mathcal{A}_{1j}\mathcal{A}_{1j} = 1, \ldots$. Then we check for orthogonality of different rows and columns ($\mathcal{A}_{1j}\mathcal{A}_{2j} = 0, \ldots$) and this may serve as a criterion of the solution admittance. Obviously the measurement uncertainties prevent exact orthogonality of the solution, and we should allow a quantitative admittance threshold $\epsilon \ll 1$. This means that given ϵ we admit only those solutions that satisfy $|\mathcal{A}_{1j}\mathcal{A}_{2j}| \leq \epsilon, \ldots$. Other solutions are rejected; this simply means that the error in the on-board determination of the solar direction and the orientation of the geomagnetic induction are too large (or inconsistent) and they cause a failure in attitude determination procedure. If ϵ is very small, we force the solution to be exact, but obviously less solutions will be obtained. Allowing higher value of ϵ we collect more solutions, but some of them would be of worse quality.

Figure 4 shows distribution of the determined Euler angles after five million trials. We have chosen $\epsilon = 0.01$ admittance level, which is partly justified by the fact that $\arcsin 0.01 \simeq 0.5$ degree (i.e. deviation of the body-frame axes from orthogonality). The resolved distributions may be approximated by a gaussian with standard deviations of 1.5 degrees (angle ψ), 0.5 degrees (angle θ) and 1.5 degrees (angle ϕ). These results are slightly worse than the assumed 0.5 degree standard deviation of the measurement noise in the satellite frame (because the inversion problem is highly nonlinear), but still they are reasonably small. Note also that the distribution in all cases is not exactly gaussian, but shows wings of rather bad solutions (again, this phenomenon is probably due to non-linearity of the procedure).

A different situation occurs, when the nutation angle θ becomes small – as pointed out above, $\theta \to 0$ is a coordinate singularity of the Euler angles.

We thus repeated our test with $\theta = 3$ degrees (and the ψ and ϕ angles as above). Results are shown in Figure 5. As expected, the nutation angle is again resolved well – its distribution is well approximated by a gaussian with the standard deviation of 0.5 degrees conformal to the chosen admittance level $\epsilon = 0.01$ – but the angles ψ and ϕ (individually) are resolved much worse. Both of them fit a gaussian distribution with the standard deviations of 8 degrees, much worse than the measurement uncertainty of 0.5 degrees. This confirms (and illustrates) that for θ small the determination of ψ and ϕ is subject to large errors. Obviously, we shall see that this drawback does not affect resolution of the satellite cross-section, which derives from knowledge of the rotation matrix $\mathcal{A}$. Components of $\mathcal{A}$ are not affected by the "singularity" of one particular representation of the rotation (Euler angles here). However, if we aim to compare the observed orientation of the satellite with predictions of a simulation that employs Euler angle parameterization (like that in Bourek 2000), we should pay attention to this problem.

Next, we may try to understand the role of the admittance-level parameter ϵ in the solution by changing its value. Figure 6 shows, as an example, statistical properties of the precession angle ψ solution when the same constants as in Figure 4 are assumed (except from ϵ). Here we compare solution with $\epsilon = 0.001$ and $\epsilon = 0.1$. As expected, the higher-ϵ solution shows worse properties (more mistaken solutions), though surprisingly the result is not that bad. The reason is due to our assumption of only 0.5 degrees uncertainty of the on-board measurements of the solar direction and the magnetic induction vector. There are only few really bad observations (at ≥ 2 degree) that would still pass through the $\epsilon = 0.1$ admittance filter and would pollute solution of the satellite attitude. We would like to point out here that this example shows importance of the reasonably small errors in the on-board measurements. Though the low-ϵ and high-ϵ solutions in Figure 6 are of a comparable quality, there is another (hidden) parameter in which the two solutions largely differ: number of solved cases. The high-ϵ solution encloses much more solved cases than the low-ϵ solution.

Figure 7 shows a fraction of admitted solutions (in percents) as a function of the standard deviation of the on-board measurement errors (σ_{BF} in degrees). Different admittance levels ϵ are considered, from $\epsilon = 0.001$ to $\epsilon = 0.05$. We may observe, that as soon as the measurement uncertainty grows above one degree, number of solved cases rapidly drops for reasonable values of ϵ. We remind that the $\arccos(\epsilon)$ parameter means minimum allowed angle between the resolved unitary vectors of the body-frame axes, or

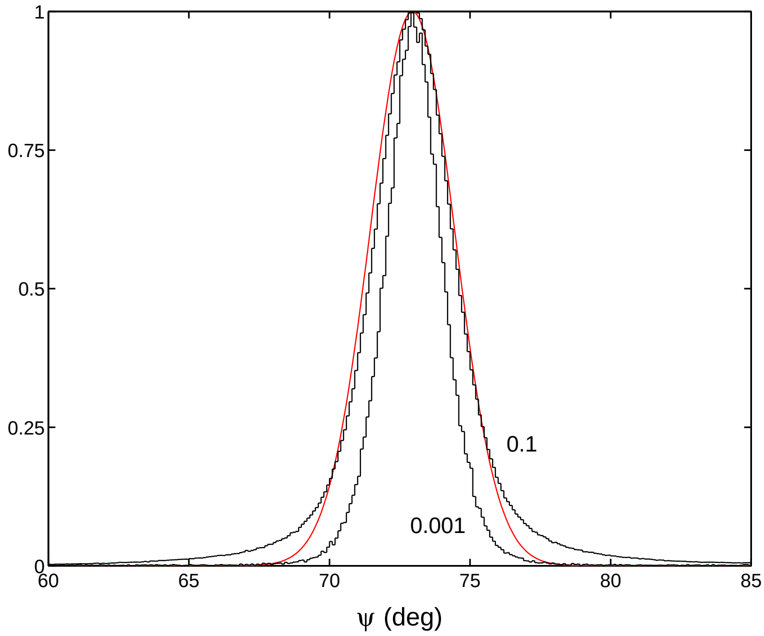

Figure 6: Determination of the precession angle ψ for different values of the admittance (ϵ); 0.5 degree standard deviation uncertainty of the on-board measurements assumed as in the previous figures. The exact (simulated) value of ψ is 73 degrees and this value is well represented by the mean value of the distribution. The $\epsilon = 0.1$ distribution of ψ is fairly well represented (apart from "wings") by a gaussian with standard deviation of 1.5 degrees.

in other words $\arcsin(\epsilon)$ is maximum allowed deviation of these angles from the right angle. For a given value of σ_{BF} (standard deviation of the uncertainty of the on-board measurements) we may thus approximately expect $\epsilon \simeq \sin \sigma_{BF}$ (thick curve on Figure 7). Indeed, for this gauge we observe approximately constant level of the solved cases (curve R). However, repeating the experiment from the Figure 6 for higher value of σ_{BF} we would notice that quality of the Euler angles determination deteriorates rapidly. This experiment again indicates necessity to care about precision of the on-board measurement system.

The rejected cases of the attitude determination ("one minus the indicated values on the Figure 7") are due to the very bad measurements that

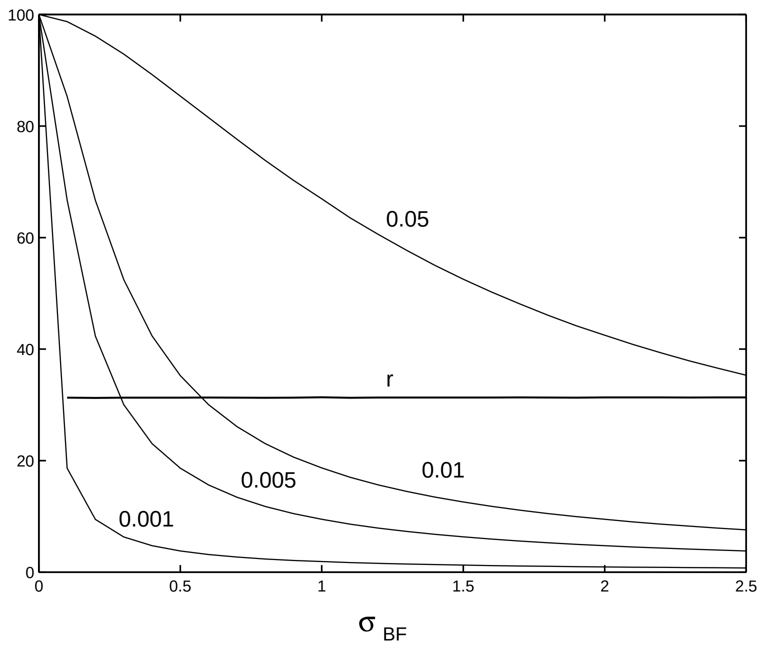

Figure 7: Percentage of the solved cases of the satellite attitude from the on-board measurements of two vectors vs their uncertainty (represented as the angular resolution σ_{BF} in degrees). Different admittance levels ϵ considered (ϵ corresponds to the label of different curves); thick curve corresponds to an approximate relation $\epsilon \simeq \sin \sigma_{BF}$.

finally cannot lead to consistent solution. Though the gaussian may represent well the measurement characteristics close to the exact (central) value, it may overestimate number of really mistaken measurements. We have thus tested a more optimistic situation with lesser amount of the bad measurements. For sake of this test we still assumed gaussian distribution near the exact value but introduced a cut-off at one sigma of this distribution (i.e. no worse measurements than one sigma from the exact value). Since this procedure rejects "bad observations" we may expect to be able to obtain higher percetange of the solved situations. Figure 8 shows the result: indeed, we can see that systematically more successful solutions of the satellite attitude have been obtained if compared to the full-gaussian case (Figure 7).

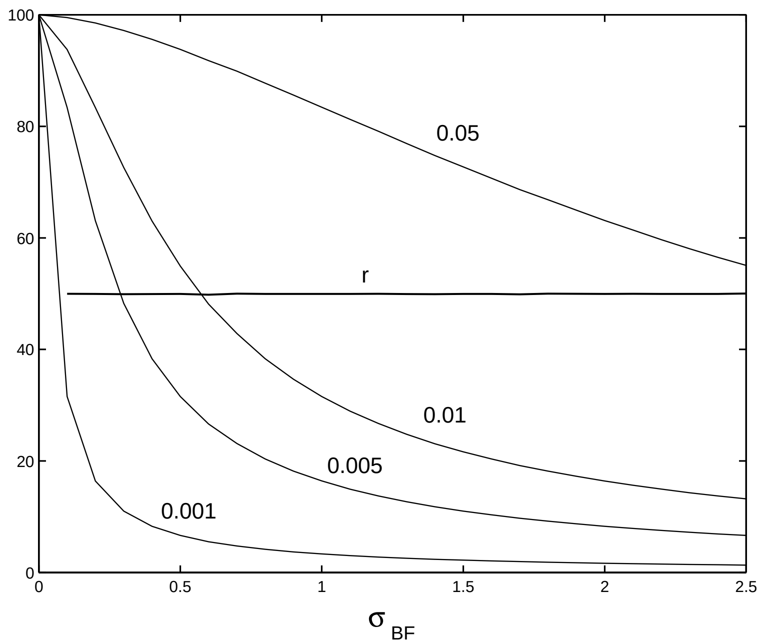

Figure 8: The same as in the Figure 7 but here we assume that none of the on-board direction measurements is worse than one sigma of the corresponding distribution. In practice we reject all simulated cases when the measurements are deviated from the exact value by more than one sigma, as if there was a sharp cut-off of the distribution ("no worse observations than σ_{BF}). The same admittance levels ϵ as in the Figure 9.

It is important to note that the laboratory measurements might reveal statistical properties of the optical and magnetometer measurements. It would be very interesting to have their results, at least as far the possible cut-off is concerned.

3.2 Cross-section of the spacecraft

The primary experimental goal of the attitude system is a possibility to determine the satellite's cross-section with respect to an arbitrary direction. Of particular importance is the cross-section perpendicular to the direction of the satellite's relative velocity with respect to the atmosphere (see Eq. (3)).

Similarly, we would like to measure the satellite's cross-section perpendicular to the geocentric position vector, which is relevant for determination of the albedo and the Earth-IR radiation effects. In the remaining part of this note we shall investigate how the uncertainties in the on-board measurements affect determination of the satellite's cross-section in the most general cases.

Since we use the same technique as above we expect that percentage of the admitted solutions does not change. We may however expect that the cross-section determination will, at least, not suffer from the coordinate singularities (like that when $\theta \to 0$ above). To that goal we have performed the following numerical experiment. We have randomly chosen orientation of the body-fixed frame of the satellite (by selecting three values of the Euler angles). As in the simulations above, we then chose two unitary vectors representing directions toward the Sun and along the geomagnetic field induction. These are represented both in the inertial frame (where we assume to know them exactly) and in the body-fixed frame. The body-fixed components are then modified by the simulated measurement uncertainty with a standard deviation of 0.5 and 2.5 degrees (for comparison). As the last step of the algorithm, we randomly selected an arbitrary direction along which we want to determine the satellite's cross-section. Since we simulate the satellite's exact attitude we may compute the exact cross-section. We also compute the cross-section from the simulated observations, but this may not correspond to the exact value because of the observational errors (whose statistical properties is also controlled in the simulation). The observationally determined cross-section is then compared with the known exact value by computing their ratio r ("determined value"/"exact value"). Since we may iterate this procedure many times (we typically perform five million trials), we may determine statistical properties of the r distribution. Results from these simulations are shown in Figure 9.

First, notice that the results on the left part of the Figure 9 (where we assumed 0.5 degree uncertainty on-board measurements) are significantly better that those on the right part of this figure (where we assumed 2.5 degree uncertainty on-board measurements). Even for high level of the admittance filter ($\epsilon = 0.1$ in this case, curve 4), which assures a high-rate of the solutions at the expense of more uncertain ones), the half–width of the r-distribution is still $\approx 0.5\%$ around unity. Also in about half of the solutions the cross-section has been determined with an error smaller than 1%. This seems to be a very good performance and tells us, empirically, that high-ϵ solution are rather well acceptable for the cross-section solution. The solutions are

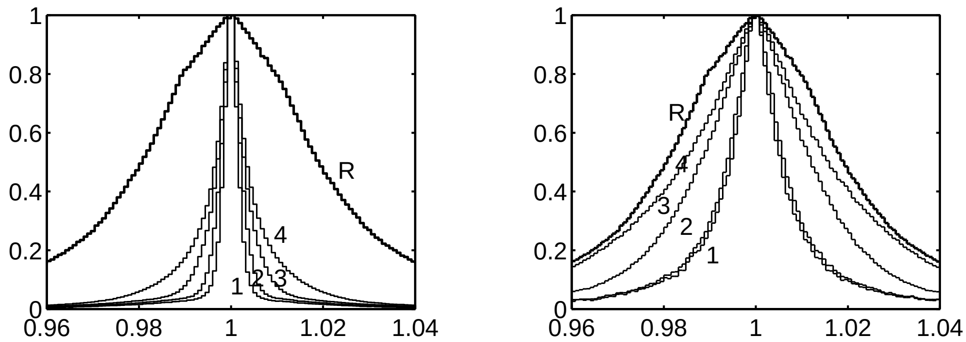

Figure 9: Statistical distribution of the r-quantity introduced in the text (ratio of the determined cross-section of the satellite and the exact cross-section). Left part assumes on-board measurements with uncertainty characterized by a standard deviation of 0.5 degrees, while the right part assumes 2.5 degrees for this quantity (low precision on-board measurements). Curves 1-4 for different values of the admittance ϵ, notably (i) $\epsilon = 0.005$ curve 1, (ii) $\epsilon = 0.01$ curve 2, (iii) $\epsilon = 0.05$ curve 3 and (iv) $\epsilon = 0.1$ curve 4. Curve labeled R corresponds to the test when, instead of solving for the satellite attitude form the on-board data, we just randomly selected the cross section according to the statistical distribution in the Figure 2.

much better than those resulting from a random selection – curves R in the Figure 9. These latter are obtained by the following procedure: rather than employing the on-board direction measurements for determination of the satellite attitude, and then computation of the cross-section, we just randomly selected two values of the cross-section according to the distribution shown in the Figure 2. One of these two values was assumed to be "true cross-section" and the other was "determined cross-section". We might thus artificially construct the r-quantity and investigate its statistical properties. Obviously, this procedure would be seriously applied only when the attitude measurements were found to be systematically corrupted or lost at all. We thus test how well we might "guess" the cross-section of the satellite by a trivial random selection. Half-width of the random-selection distribution is about 2% and half-cases is about 3% off the unity. This, after all not that bad, result is obviously due to peculiar shape of the satellite cross-section distribution in the Figure 2 that is sharply peaked (much higher or smaller

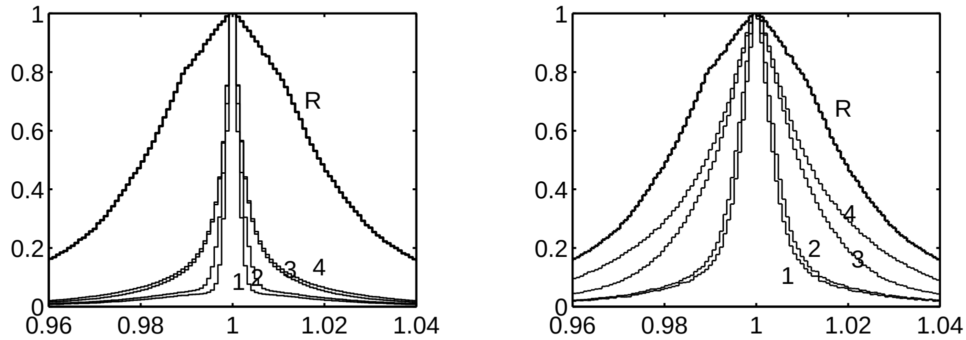

Figure 10: The same as in the Figure 9 but here a cut-off at one sigma of the gaussian distribution of the modelled observational errors has been introduced (as in the Figure 8).

values are the marginal and not very likely to occur).

When the on-board measurements are of lower quality – as in the right part of Figure 9 where we assumed 2.5 degree uncertainty of the measurements – the cross-section of the satellite gets determined worse. The high-ϵ solutions are even comparable to the random shooting described above and thus we may conclude that the whole procedure of the observational determination of the satellite cross-section is, from the statistical point of view, useless exercise. This result thus again points out importance of the high-quality of the on-board measurements.

A little better results are obtained when the measurements errors are cut at the sigma of the assumed gaussian distribution (and thus the really bad observations of the gaussian tail above the standard deviation are not modelled). Figures 10 show these results. The left part resembles that of the Figure 9, while the right indicates improved results when low admittance filter (i.e. high-ϵ) is allowed. In general, however, the results in the Figures 9 and 10 are not significantly different.

Results in this section allow us to formulate the following important conclusion: bad performance of the on-board attitude measurement system (uncertainty ≈ 2.5 degree and worse) and high solution rate (high ϵ) allows only very poor determination of the satellite cross-section approximately equivalent to its random selection; high performance of the on-board attitude measurement system (uncertainty ≈ 0.5 degree or better) with even high solution rate requirement (high ϵ) allows very good determination of the satellite cross-section (significantly better than the random selection). It is thus important to maintain the subdegree precision of the on-board measurements of the solar position and the direction of the geomagnetic field.

4 Conclusions

The main results of this study may be summarized as follows:

- We have performed a likelihood analysis of MIMOSA cross-section (assuming the direction from which the satellite is seen to be random in space); the minimum and maximum values of the cross-section were found as well as the statistical distribution of the cross-section for the intermediate values. This latter was found non-uniform, with a significant peak at about 0.2623 m^2. As indicated in the last Section 3.2, this value may be considered as a zero approximation for the MIMOSA cross-section when the satellite attitude is not resolved; random selection of the satellite's cross-section results staistically in about 2% mismatch of this quantity.

- Satellite's cross-section perpendicular to the solar direction may be generally resolved very well. Even a low-quality on-board optical measurements seem to assure approximately 1% (or better) uncertainty in this quantity. Determination of the direct solar radiation pressure seems to be affected more significantly by the imperfect knowledge of the optical properties of the satellite surface (specular and diffuse reflectivity coefficients). Precise laboratory tests may be thus welcome to constrain the error in the solar radiation pressure determination (important for the space calibration of the accelerometer).

- The uncertainty analysis indicates that a half-degree (or better) uncertainty in the measurements of the body fixed orientation toward the Sun and of the geomagnetic field is required to assure a success in the attitude determination of the satellite; larger uncertainties would result in too many rejections and bad performance in determination the satellite cross-section.

- This study might profit from the precisely documented performance of the on-board optical system for determination of the solar direction and the magnetometer measurements of the geomagnetic induction vector. By this we mean understanding the statistical distribution of the measurement errors (here we have assumed a gaussian, or a gaussian with and artificial cut-off, distributions).

- Further investigation of the method used for the attitude determination (in particular search for the optimum set of variables) and tuning the attitude determination software might be desirable in the future.

This note is a part of documents prepared for the Czech Grant Agency contract 205/96/K119.

References

[1] V.V. Beletskii and A.M. Yanshin, *Influence of the Aerodynamical Effects on Rotational Motion of the Artificial Satellites*, Naukova-Dumka, Kiev (1984)

[2] P. Bourek, Rotational dynamics of the satellite MIMOSA, Dissertation, Charles University, Prague (2000)

[3] I.K. Harrison and G.G. Swinerd, Analysis of satellite laser ranging data to investigate satellite aerodynamics, *Planet. Sp. Sci.* **43**, 1023–1033 (1995)

[4] D. King-Hele, *Theory of Satellite Orbits in an Atmosphere*, Butterworths, London (1964)

[5] H. Klinkrad, B. Fritsche and A. Kashkovsky, Modelling of non-gravitational forces for low-Earth orbits, presented at 50th IAF meeting, Amsterdam (1999)

[6] V.N. Koshlyakov, *Dynamics of Solid Bodies and Applied Theory of Tops*, Nauka, Moscow (1985)

[7] F. Mignard, Mouvement du solide, in: *Modern Methods of Celestial Mechanics*, eds. D. Benest and C. Froeschlé, Ed. Frontieres, Gif-sur-Yvette (1990)

[8] MIMOSA, Zpráva o výsledcích k oponentuře komplexního projektu GAČR 205/96/K119, ed. L. Sehnal, Prague (Sept 1998)

[9] L. Sehnal, Determination of satellite drag coefficient from the orbital analysis of the ANS satellite (1974-70A), *Bull. Astron. Inst. Czechosl.* **33**, 244–249 (1982)